Grafting of Benzylic Amide Macrocycles onto Acid-Terminated Self-Assembled Monolayers Studied by XPS, RAIRS, and Contact Angle Measurements

Francesca Cecchet,[†] Michael Pilling,[†] Laszlo Hevesi,[‡] Stefano Schergna,[§] Jenny K. Y. Wong,[||] Guy J. Clarkson,[§] David A. Leigh,[⊥] and Petra Rudolf*[,†]

Laboratoire Interdisciplinaire de Spectroscopie Electronique and Chimie des Matériaux Organiques, Facultés Universitaires Notre-Dame de la Paix, 61 rue de Bruxelles, B-5000 Namur, Belgium, Centre for Supramolecular and Macromolecular Chemistry, Department of Chemistry, University of Warwick, Gibbet Hill Road, Coventry CV4 7AL, United Kingdom, and School of Chemistry, University of Edinburgh, West Mains Road, Edinburgh EH9 3JJ, United Kingdom

Received: November 7, 2002; In Final Form: June 24, 2003

The grafting of benzylic amide macrocycles, the basic units of more complex mechanically interlocked architectures such as catenanes and rotaxanes, was performed via the functionalization of an acid-terminated self-assembled monolayer (SAM) of 11-mercaptoundecanoic acid (11-MUA). Both chemical and physical adsorption were investigated using macrocycles containing either a reactive hydroxyl functionality or an *exo*-pyridyl moiety, with characterization of the systems using X-ray photoelectron spectroscopy (XPS), contact angle measurements, and reflection absorption infrared spectroscopy (RAIRS). By comparing theoretical values with experimental data, it was found that up to 40% of the acid groups on the SAM surface were modified by the macrocycles and that the macrocycle coverage can be controlled by varying the reaction time. Stability tests demonstrated that the prepared films are stable in air, under ultrasound treatment and against chemical substitution. RAIRS measurements suggested a tilted orientation of the macrocycle with respect to the plane of the SAM surface.

1. Introduction

Considerable interest has been focused on the preparation and characterization of functionalized, switchable, ordered arrays of mechanically interlocked molecules for the purpose of developing new and promising multifunctional materials.[1−3] Catenanes and rotaxanes, two classes of interlocked molecules, have shown great potential as components for nanoscale devices in the form of molecular shuttles, switches, and information storage systems.[4−7] The key property of catenanes (two or more mechanically interlocked macrocycles) and rotaxanes (one or more macrocycles locked onto a linear "thread" by two bulky terminal stoppers) is that the mechanical bond holding the components of the molecule together allows large-amplitude relative movements of the components and can be used to modify the molecular properties by external stimuli.[8−12] Ideally, the incorporation of these molecules into workable devices involves the formation of ordered bidimensional arrays while retaining their dynamic properties.

Functionalization of alkanethiol SAMs is a method often used to anchor macromolecular units such as proteins or enzymes onto a solid surface (see, for example, refs 13−24). The success of this approach is due to the simplicity of SAM film preparation, its reproducibility, and the possibility to create a wide range of surfaces via the incorporation of different groups at the end of the alkyl chains at the gas− or liquid−monolayer interface. The use of SAMs as a starting point for building more complex molecular architectures provides the possibility of grafting different types of molecules onto a surface. This grafting method has several advantages: it preserves the chemical, physical, or biological properties of the attached molecules, it allows the distance between the molecules and the surface to be varied, and the parameters of the process of functionalization can be controlled. There are two basic functionalization approaches; the first involves chemical modification via covalent bonding between a molecule and the SAM, and in the second method, the molecule is physisorbed onto the SAM and held in place by electrostatic or hydrogen bonding interactions.

Considering the complex molecular structures of catenanes and rotaxanes, we chose to identify the conditions and the parameters necessary for anchoring these molecules onto SAMs starting from a study of a single-component system comprising only the macrocycle. In this work, we investigated two different types of macrocycles shown in Figure 1a and b: **1** containing a hydroxyl group and **2** containing a pyridine function. As illustrated in Figure 2, macrocycle **1** is expected to react with the acid-terminated monolayer, which has been activated by the 1-(3-dimethylaminopropyl)-3-ethylcarbodiimide hydrochloride (EDCI), to form a covalent bond with the SAM. Macrocycle **2** should bind to the SAM through an electrostatic or hydrogen bonding interaction and hence be physisorbed.

2. Experimental Section

Materials. Macrocycles **1** and **2** (Figure 1a and b) were synthesized using methods analogous to those previously

* Corresponding author. Current address: Materials Science Centre, University of Groningen, Nijenborgh 4, 9747 AG Groningen, The Netherlands. E-mail: p.rudolf@phys.rug.nl. Fax: +(31)50-363 4879.

[†] Laboratoire Interdisciplinaire de Spectroscopie Electronique, Facultés Universitaires Notre-Dame de la Paix.

[‡] Chimie des Matériaux Organiques, Facultés Universitaires Notre-Dame de la Paix.

[§] University of Warwick.

[||] University of Edinburgh.

[⊥] Contact for materials. E-mail: david.leigh@ed.ac.uk. Fax: +44-131-667-9085.

10.1021/jp022380b CCC: $25.00
Published on Web 09/09/2003

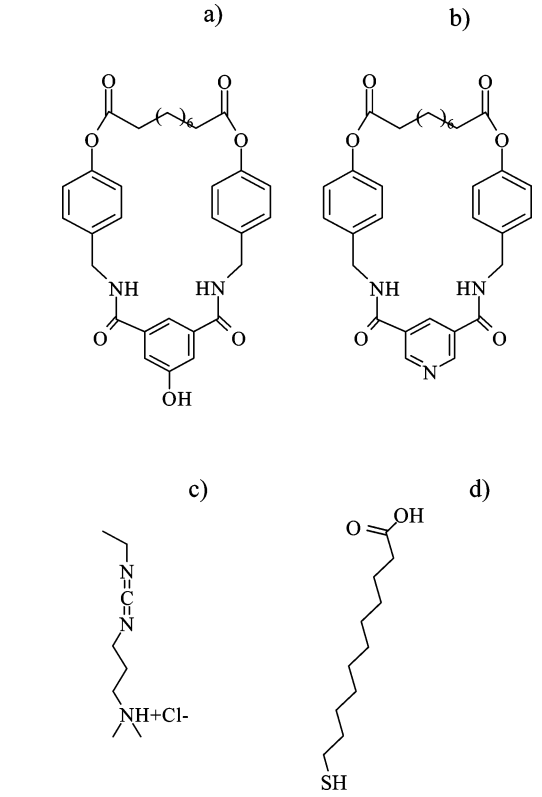

Figure 1. Simplified representation of (a) macrocycle **1** containing a hydroxyl functionality, (b) macrocycle **2** containing an *exo*-pyridyl moiety, (c) 1-(3-dimethylaminopropyl)-3-ethylcarbodiimide hydrochloride (EDCI), and (d) 11-mercaptoundecanoic acid (11-MUA).

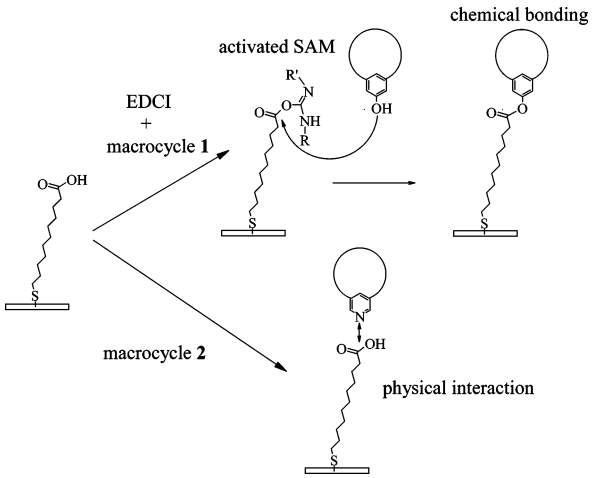

Figure 2. Schematic representation of the functionalization process of an 11-MUA self-assembled monolayer with macrocycles **1** and **2**.

described in the literature.[10] 1-(3-Dimethylaminopropyl)-3-ethylcarbodiimide hydrochloride (98+%, Aldrich) (Figure 1c), 11-mercaptoundecanoic acid (95%, Aldrich) (Figure 1d), chloroform, and dichloromethane (HPLC grade, Acros) were used as supplied.

Preparation of Monolayers. The substrates were gold films evaporated on Si(111) wafers (IMEC, Belgium). They were cleaned in an ozone discharge for 15 min, followed by sonication in ethanol for 20 min immediately before being employed. Carboxylic acid-terminated SAMs were prepared by immersing the gold substrates in a 1 mM chloroform solution of 11-MUA for 21 h. The samples were rinsed in chloroform and dried under argon before characterization by XPS (X-ray photoelectron spectroscopy), RAIRS (reflection absorption infrared spectroscopy) and contact angle measurements.

Functionalization Using Macrocycles 1 and 2. To graft macrocycle **1**, the carboxylic acid-terminated SAMs were immersed in 1 mM solutions (using dichloromethane as the solvent) of EDCI and **1** for 7 to 118 h. The grafting of macrocycle **2** took place over the same immersion times using a 1 mM dichloromethane solution of **2**. Films of 11-MUA derivatized with EDCI alone were prepared by immersion in a 1 mM aqueous solution for 51 h.[25] The modified surfaces were each rinsed and sonicated for 30 s in the pure solvent (dichloromethane or water) and dried under a stream of argon prior to analysis by XPS, RAIRS and contact angle measurements.

Stability Tests. The stability of the films was investigated upon exposure to ultrasound treatment for 30 s to 20 min. Their stability against aging under atmospheric conditions was verified by exposing the films to air for 3−20 days. To avoid light-induced aging effects, the films were kept in the dark during these stability tests. The SAM film functionalized with macrocycle **2** was also checked against chemical substitution by exposing it to molecules that can also physisorb onto the surface and therefore potentially displace the macrocycle. The films were exposed to either a 15 mM aqueous solution of ammonium chloride, a 1 mM methanol solution of aniline, or a 10 mM methanol solution of aniline for different immersion times and then rinsed in the pure solvent before analysis. Before and after each treatment, the surfaces were characterized by XPS and contact angle measurements.

X-ray Photoelectron Spectroscopy (XPS) Analysis. High-resolution XPS measurements were performed using an SSX-100 (Surface Science Instruments) photoelectron spectrometer with a monochromatic Al Kα X-ray source ($h\nu = 1486.6$ eV). The energy resolution was set to 0.92 eV, and the photoelectron takeoff angle (TOA) was 90°. All binding energies were referenced to the Au $4f_{7/2}$ core level.[26] The base pressure in the spectrometer was in the low 10^{-10} Torr range.

Spectral analysis included a linear background subtraction and peak separation using mixed Gaussian−Lorentzian functions in a least-squares curve-fitting program (Winspec) developed in our laboratory. The photoemission peak areas of each element, used to estimate the amount of each species on the surface, have been normalized by the sensitivity factors of each element tabulated for the spectrometer used.

Three different points of each sample were analyzed to check for homogeneity. Within the error bars quoted, we found the same atomic proportions for all points of the same sample and therefore conclude that all samples can be considered homogeneous.

Contact Angle Measurements. Static contact angles of deionized (milli-Q) water deposited on the samples were measured in air using a video contact angle system VCA-2500XE (AST Products). All quoted angles are subject to an error of ±3°.

Reflection Absorption Infrared Spectroscopy (RAIRS). The RAIRS experiments were performed at room temperature in the sample compartment of a Biorad FTS-60A FT-IR spectrometer. P-polarized infrared radiation was reflected from 11-MUA SAM films functionalized with macrocycle **1** at an 85° angle of incidence with respect to the surface normal and detected with a liquid-nitrogen-cooled MCT detector. Data were recorded as the coaddition of 256 scans in single-beam mode at resolutions of up to 2 cm^{-1}, and the final spectrum was obtained with a minimum of baseline correction. The RAIRS

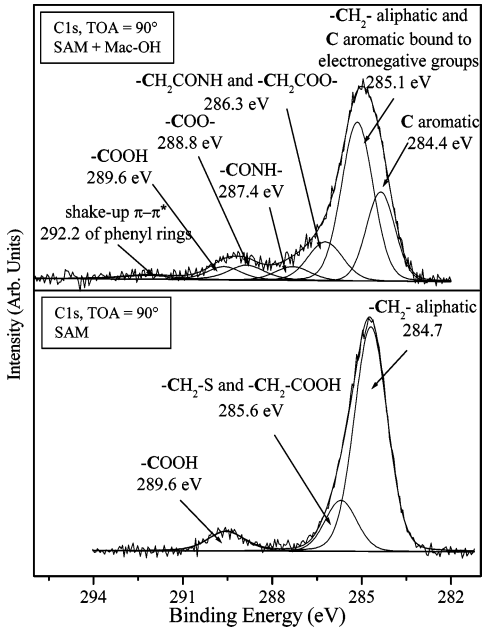

Figure 3. Photoemission spectra and fit of the C 1s core-level region for an 11-MUA film (bottom panel) and an 11-MUA film functionalized with macrocycle **1** (top panel).

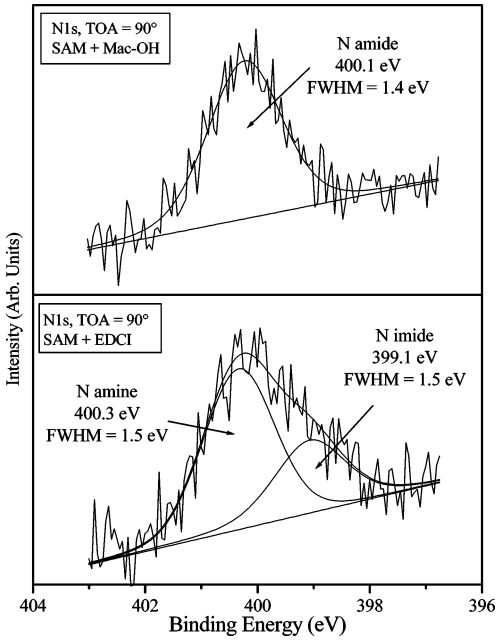

Figure 4. Photoemission spectra and fit of the N 1s core-level region for an 11-MUA film functionalized with EDCI (bottom panel) and for an 11-MUA film functionalized with macrocycle **1** (top panel).

spectra are displayed as the ratio of the adsorbed macrocycle single beam to the single beam of 11-MUA on gold. In addition to the RAIRS measurements, infrared transmission spectra of solid-state macrocycle **1** were recorded using 150-mg pellets, 1 wt % of the macrocycle in KBr. Data collection conditions were similar to those used for the RAIRS experiments but with the spectrometer in transmission mode.

3. Results and Discussion

XPS Analysis. a. SAM Functionalization with Macrocyle 1. *Characterization of the Modified Surfaces*. Figure 3 shows the carbon 1s core-level photoemission spectra for a SAM of 11-MUA (bottom panel) and for a SAM functionalized with macrocycle **1** (top panel). Because no chlorine could be detected in the photoemission spectra of these samples (not shown), we can be sure that no solvent molecules (CH_2Cl_2) are incorporated into the layers and that the C signals are due solely to the molecules in question. From the spectral analysis of the experimental data of the SAM (Figure 3 bottom panel), the first peak at 284.7 eV is assigned to the aliphatic carbons of the alkyl chains. The signal due to carbons bound to sulfur and the acid group is found at 285.6 eV, and the last peak at 289.6 eV corresponds to the carboxylic carbon.[27,28] Figure 3 (top panel) shows the carbon 1s core-level region of the SAM activated by the EDCI after 51 h of reaction with macrocycle **1**. Although there are 14 or 15 chemically distinct carbon environments in this film, in practice XPS cannot distinguish between all 7 types of phenyl-ring carbons in **1** or between the 5 different types of aliphatic carbons. Hence, the spectral analysis procedure consists of fitting a minimum number of peaks consistent with the raw data and the molecular structure of the film, with the simplification of assuming equivalent carbon atoms depending on their environment. Figure 3 (top panel) illustrates a fit of the experimental data assuming a molecular structure with six chemically shifted C 1s core-level photoemission peaks. It is immediately apparent that there are several differences between the spectrum recorded for the SAM and the derivatized SAM. The first peak at 284.4 eV, unambiguously assigned to aromatic carbon, confirms the presence of the macrocycle. The peak at 285.1 eV originates from different contributions, namely, from carbon atoms of the aliphatic chains both on the macrocycle (Figure 1a) and on the thiol and from aromatic carbon atoms bound to electronegative groups. This explains why its intensity is also important after functionalization by **1.** At the higher binding energy of 286.3 eV, a component due to aliphatic carbon atoms bound to electronegative carboxylic and amide groups is identified. Peaks characteristic of amide, ester, and carboxylate carbons are observed at 287.4, 288.8, and 289.6 eV, respectively. Finally, the shake-up feature associated with the aromatic rings is found at 292.2 eV.[29,30]

The most convincing evidence that macrocycle **1** is present on the surface comes from the analysis of the photoemission spectra of the nitrogen 1s core-level region. In the spectra recorded for the monolayer functionalized by the macrocycle, shown in Figure 4 (top panel), the single peak at 400.1 eV binding energy with a full width at half-maximum (fwhm) of 1.4 eV corresponds to the amide nitrogen.[29,30] We can exclude the possibility that this signal comes from the nitrogen atoms of EDCI by comparing the N 1s core-level spectrum recorded for the macrocycle with that recorded for the monolayer activated by EDCI alone (Figure 4, bottom panel). The N 1s core-level photoemission line of the EDCI film shows two components, at 399.1 eV (fwhm = 1.5 eV) and 400.3 eV (fwhm = 1.5 eV) binding energy, assigned to imine and the amine nitrogen of EDCI. The peak-area ratio of these two components is 1:2, as expected from the chemical composition of EDCI, in contrast to the single component due to the amide nitrogen recorded for the macrocycle films. Incidentally, we note that the value of binding energies in the N 1s spectra of the EDCI film points to a deprotonated EDCI on the surface. Indeed, for the protonated species, one expects a higher binding-energy value for amine nitrogen. This agrees with the fact that no Cl has been detected on this sample (i.e., H^+Cl^- remains in solution). Even in the N 1s spectra recorded for samples corresponding to shorter immersion times (not shown) we find exactly the same line shape as that shown in Figure 4 (top panel), whereas if we expose the EDCI film to a solution containing only the macrocycle, we find afterward an N 1s spectrum (not

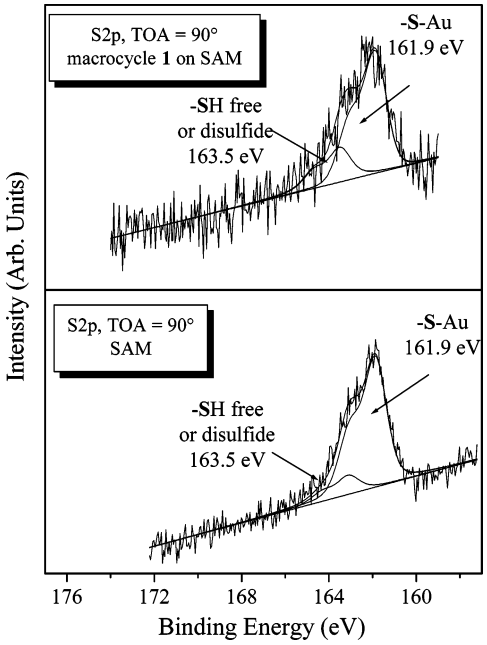

Figure 5. Photoemission spectra and fit of the S 2p core-level region for an 11-MUA film (bottom panel) and for an 11-MUA film functionalized with macrocycle **1** (top panel).

shown) very similar to the EDCI N signal, which can be reproduced by adding to the spectrum of Figure 4 (bottom panel) a tiny amount of the spectrum Figure 4 (top panel). This indicates that when the entire surface is covered by EDCI very few active sites on the SAM are accessible to the macrocycle.

When instead EDCI and the macrocycle are present in the solution to which the SAM is exposed, the activation of a site by the EDCI is followed by its functionalization until all of the available sites are functionalized, and this explains why no EDCI signal is present in the N 1s spectrum of film functionalized with **1** (Figure 4, top panel).

Figure 5 presents the S 2p photoemission lines of the SAM before (bottom panel) and after (top panel) functionalization with the macrocycle. The latter signal is weaker (hence showing more noise), as expected for a thicker film, indirectly confirming the macrocycle's presence. However, it is still possible to identify, as for the SAM alone (Figure 5, bottom panel), two components. For the first, the S $2p_{3/2}$ peak is situated at 161.9 eV, and we assign it to sulfur bonded to gold.[26,31] The other component with the S $2p_{3/2}$ peak at 163.5 eV could be due to a small number of alkanethiols not covalently bonded to the substrate but only intercalated between the 11-MUA molecules bound to Au or physisorbed as a double layer.[26,31] Alternatively, the second component might be derived from disulfides formed under the influence of X-rays during spectra acquisition.[33] We cannot discriminate between these contributions because we do not see any changes indicative of more X-ray-induced degradation when we compare spectra taken with 2 h (shown in the Figure) and 8 h of irradiation, contrary to what is reported in ref 33. However, the aging behavior of the films supports the disulfide attribution. (See Stability of the Films below.)

Estimation of the Functionalization Yield. Figure 6a shows a plot of the ratios between the N 1s and S 2p (top panel), N 1s and Au 4f (center panel), and S 2p and Au 4f (bottom panel) photoemission peak areas as a function of the reaction time. As expected, the S 2p to Au 4f ratio remains reasonably constant for all immersion times, indicating that the monolayer of 11-MUA is stable under these conditions. The N 1s to Au 4f and N 1s to S 2p ratios increase with the immersion time, indicating

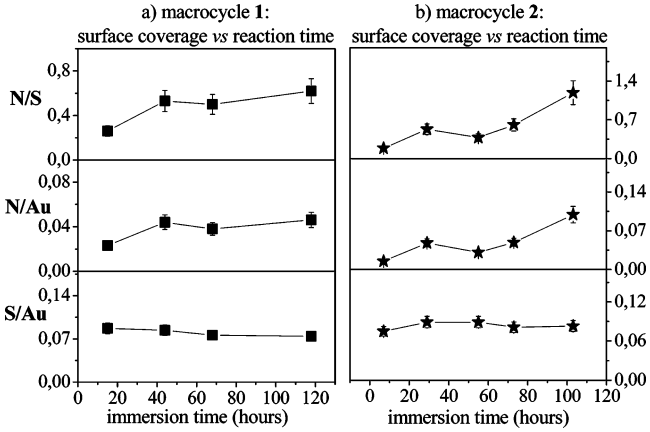

Figure 6. Experimental atomic ratios derived from the photoemission peak areas of sulfur and gold (bottom panel), nitrogen and gold (center panel), and nitrogen and sulfur (top panel) as a function of the reaction time recorded (a) for an 11-MUA film functionalized with **1** and (b) for an 11-MUA film functionalized with **2**. The error in the atomic ratio was estimated to be 10% for S/Au, 15% for N/Au, and 18% for N/S, assuming there is no significant error in the Au $4f_{7/2}$ photoemission peak area.

TABLE 1: Comparison between Experimental Atomic Percentages Derived from the Photoemission Peak Areas of an 11-MUA Film Functionalized with Macrocycle 1 Prepared with Different Increasing Immersion Times and Theoretical Values Calculated for Different Coverages[a]

	15 h exp	68 h exp	118 h exp	12% theor	30% theor	50% theor
%C	76.5 ± 1.5	77.9 ± 1.6	77.4 ± 0.2	78.9	79.2	79.4
%O	16.2 ± 0.8	14.7 ± 0.7	15.7 ± 0.8	14.5	14.6	14.7
%S	5.8 ± 0.6	5.0 ± 0.5	4.3 ± 0.4	5.3	3.8	2.9
%N	1.5 ± 0.2	2.5 ± 0.4	2.7 ± 0.4	1.3	2.3	2.9
N/S	0.3 ± 0.1	0.5 ± 0.1	0.6 ± 0.1	0. 25	0.6	1

[a] The error in the experimental atomic percentages was estimated to be 2% for C, 5% for O, 10% for S, and 15% for N.

macrocycle adsorption. We also compared the experimentally determined atomic percentages, obtained from the photoemission peak areas, with those calculated for the functionalization of 12, 30, and 50% of the acid groups of the SAM. In the calculation, we considered a model surface of 100 thiol chains and computed the atomic percentages for N, C, O, and S (excluding hydrogen, which cannot be detected by XPS) for a coverage of 12, 30, or 50 macrocycle molecules.[32] The results are summarized in Table 1: after 15 h of reaction, 12% of the surface acid groups are functionalized by **1,** while after 118 h a yield of 30% is reached. Comparing the size of an acid group to the dimensions of a macrocycle (average diameter 10 Å) and considering that the orientation of the macrocycle with respect to the surface may be random, we can conclude that nearly all of the self-assembled monolayer area is covered by macrocycle **1**.

The error in the photoemission peak areas was estimated depending on the signal-to-noise ratio in the spectrum for each element: the carbon and oxygen signals are better defined because the errors were found to be 2 and 5%, respectively. The sulfur and nitrogen signals are weaker, producing a noisier experimental curve and therefore more substantial errors in the peak area, estimated at 10 and 15%, respectively. Unfortunately, the films degraded upon prolonged X-ray irradiation, as often observed for organic layers,[33−35] and it was therefore not possible to increase the accumulation time, which would have provided a better signal-to-noise ratio.

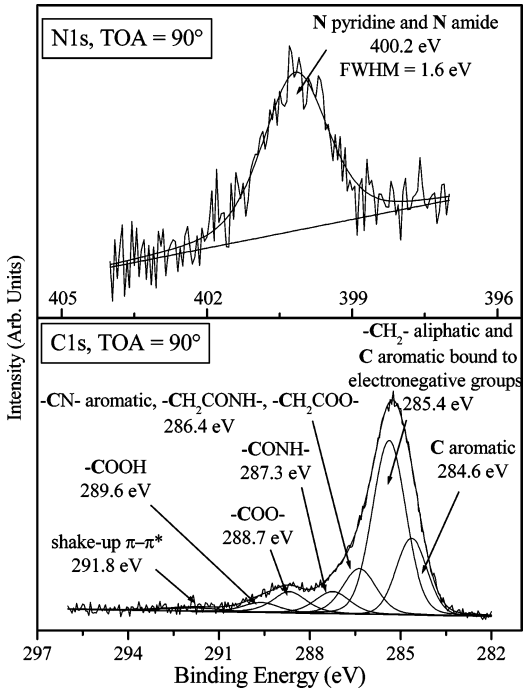

Figure 7. Photoemission spectra and fit of the C 1s (bottom panel) and N 1s (top panel) core-level regions for an 11-MUA film functionalized with macrocycle **2**.

b. SAM Functionalization with Macrocyle 2. *Characterization of the Modified Surfaces.* As for macrocycle **1**, the changes induced by the functionalization of the 11-MUA SAM with macrocycle **2** was followed by XPS. Figure 7 shows the N 1s and C 1s core-level regions in detail as well as their components deduced from the spectral analysis. First, the appearance of a photoemission signal in the N 1s core-level region (Figure 7, top panel) confirms the presence of the macrocycle on the surface of the acid-terminated SAM. The large peak at 400.2 eV (fwhm = 1.6 eV) is due to amide nitrogen atoms and to the pyridine nitrogen in the macrocycle. The C 1s core-level spectrum for the functionalized monolayer (Figure 7, bottom panel) shows a peak at 284.6 eV due to aromatic carbons and one at 285.4 eV corresponding to the aliphatic chain and to aromatic carbon atoms bound to electronegative groups. In addition, the shoulder at 286.4 eV comprises the C1s signal of aliphatic carbon atoms bound to carboxylic or amide groups and to pyridine nitrogen. At 287.3 eV, we find the signature of amide carbon, at 288.7 eV, that of ester carbon, and at 289.6 eV, that of carboxylate carbon. The last feature at 291.8 eV is the shake-up associated with the aromatic rings.[29,30]

In considering the interaction between the SAM and macrocycle **2**, pyridine N 1s photoemission is expected between 399.0 and 399.5 eV depending on the chemical environment of the pyridine rings.[36] However, theoretical calculations on catenanes investigating the effects of intra- and intermolecular interactions on the binding energy showed that hydrogen bonding interactions can produce shifts to higher binding energy of up to 1 eV.[37] An electrostatic interaction between a protonated pyridine nitrogen and an anionic carboxylate function following the exchange of the proton of the carboxylic acid group should give rise to a new component in the N 1s core-level region between 401.0 and 402.0 eV,[36] which is not seen. We can therefore rationalize the fact that we do not distinguish two separate components for amide and pyridine nitrogen in the N 1s core level (Figure 7, top panel) by assuming that the interaction between the pyridine moiety of the macrocycle and the acid group of the SAM does not occur through proton exchange but through hydrogen bonding, at least for the large majority of molecules.

TABLE 2: Comparison between Experimental Atomic Percentages Derived from the Photoemission Peak Areas of an 11-MUA Film Functionalized with Macrocycle 2 Prepared with Different Increasing Immersion Times and Theoretical Values Calculated for Different Coverages[a]

	7 h exp	24 h exp	103 h exp	10% theor	30% theor	40% theor
%C	76.7 ± 1.5	77.4 ± 1.5	75.6 ± 1.5	78.3	78.1	78.0
%O	17.1 ± 0.9	15.9 ± 0.8	16.5 ± 0.8	14.4	14.6	14.7
%S	5.2 ± 0.5	3.6 ± 0.4	3.6 ± 0.4	5.6	3.8	3.3
%N	1.0 ± 0.2	3.2 ± 0.5	4.3 ± 0.6	1.7	3.5	4.0
N/S	0.2 ± 0.0	0.9 ± 0.2	1.2 ± 0.2	0.3	0.9	1.2

[a] The error in the experimental atomic percentages was estimated to be 2% for C, 5% for O, 10% for S, and 15% for N.

Estimation of the Functionalization Yield. Similar to the procedure detailed above for **1**, we followed the evolution of the functionalized surface as a function of the immersion time by XPS. Figure 6b shows the ratios between the photoemission peak areas of N 1s and S 2p (top panel), N 1s and Au 4f (center panel), and S 2p and Au 4f (bottom panel) versus time. The S 2p to Au 4f ratio remains constant for all immersion times, confirming the stability of the SAMs, as observed for **1**. The N 1s to Au 4f and N 1s to S 2p ratios increase with the immersion time from 7 to 103 h, indicating a gradual increase in the functionalized surface area. Moreover, a comparison of the experimental atomic percentages obtained from the peak area with the theoretical values calculated as explained previously for **1** and shown in Table 2 indicates that after 7 h of immersion 10% of the acid groups of the SAM are functionalized by **2** and after 103 h of immersion the functionalization yield reaches 40%. As for **1**, we note that on the basis of the dimensions of both the acid groups and **2** this corresponds to a value close to the maximum possible surface coverage.

We note that the functionalization yields for **1** and **2**, determined as detailed above, rely on the implicit assumption that the SAM is compact and no free gold surface is available for direct adsorption. Deducing reliable information on the compactness and the thickness of both the SAM of 11-MUA and the SAM functionalized with either **1** or **2** from the XPS data is extremely difficult because precise values for the electron escape depth are not available.[38] We therefore decided to approach the problem through a completely independent series of electrochemical experiments. The results of this work are too copious to be included here, and we are currently preparing a separate manuscript detailing them.[39] However, we found evidence of a highly ordered and compact SAM (no holes or defects).

c. Stability of the Films. More detailed information on the type of bonding interactions between the macrocycles and the 11-MUA SAM would be of great interest and is contained within the C 1s photoemission signal. However, because of the complexity of this core-level region consisting of multiple components, it was not possible to prove the exact nature of the interaction between the macrocycle and the acid-terminated SAM surface by XPS. Nevertheless, photoemission can be used to investigate the stability of the macrocycle-functionalized SAMs under different external conditions such as ultrasound treatment and aging in air. Contact angle measurements were performed to distinguish the different surfaces by their polarity, and XPS allowed us to monitor possible chemical changes.

The contact angle (CA) obtained for the 11-MUA SAM immediately after deposition of the drop is 29°; however, during

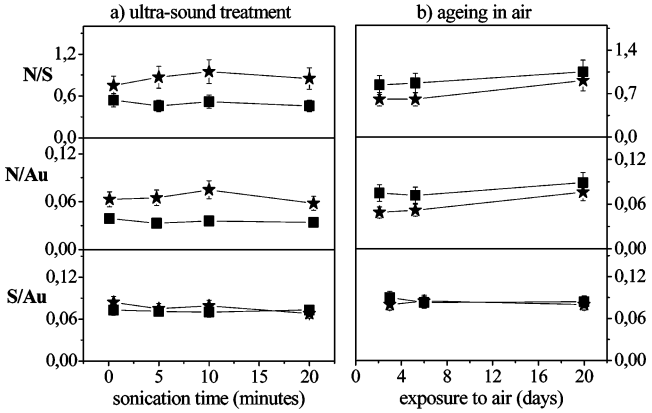

Figure 8. Experimental atomic ratios derived from the photoemission peak areas of sulfur and gold (bottom panel), nitrogen and gold (center panel), and nitrogen and sulfur (top panel) recorded for an 11-MUA film functionalized with macrocycle **1** (−■−) and macrocycle **2** (−★−) (a) as a function of the ultrasound treatment time and (b) as a function of the aging time in air. The error in the atomic ratio was estimated to be 10% for S/Au, 15% for N/Au, and 18% for N/S, assuming there is no significant error in the Au $4f_{7/2}$ photoemission peak area.

TABLE 3: Comparison between Experimental Atomic Percentages Derived from the Photoemission Peak Areas of an 11-MUA Film Functionalized with Macrocycle 1 Freshly Prepared and after Aging in Air[a]

	freshly prepared	3 days	6 days	20 days
%C	80.5 ± 1.6	74.9 ± 1.5	75.4 ± 1.5	74.7 ± 1.5
%O	13.1 ± 0.7	18.2 ± 0.9	17.9 ± 0.9	19.4 ± 1.0
%S	3.3 ± 0.3	3.8 ± 0.4	3.4 ± 0.3	2.9 ± 0.3
%N	3.1 ± 0.5	3.2 ± 0.5	3.0 ± 0.5	3.0 ± 0.5
N/S	0.9 ± 0.2	0.8 ± 0.1	0.8 ± 0.1	1.0 ± 0.2

[a] The error in the experimental atomic percentages was estimated to be 2% for C, 5% for O, 10% for S, and 15% for N.

the following minute, the drop wets the surface, and the contact angle drops below 10°, as expected for such a highly hydrophilic surface.[40] The reaction of EDCI with the acid groups of the SAM according to the scheme in Figure 2 increases the CA to 76°, indicating that a more hydrophobic surface has been produced. After reaction of the SAM activated by EDCI with **1**, a CA of 55° confirms the presence of the macrocycle, whose amide and ester groups are responsible for the more hydrophilic character of the surface. Because **1** and **2** are very similar, it is not surprising that we find a CA of 57° after functionalization of the SAM with the latter. Macrocycle films subjected to ultrasound treatment showed the same contact angle values even after 20 min of treatment. Figure 8a shows the N 1s to S 2p, N 1s to Au 4f, and S 2p to Au 4f ratios calculated from the XPS peak areas for the same films of **1** and **2** after sonication; these ratios are constant for all sonication times in agreement with the contact angle data, confirming that macrocycle-functionalized SAMs are stable with respect to ultrasound treatment.

To monitor changes due to aging in the dark, XPS spectra of films of SAMs functionalized with **1** and **2** were collected after exposure to air for 3, 6, and 20 days. The atomic percentages calculated from these spectra for **1** are shown in Table 3; an increase in the amount of oxygen on the surface is clearly seen after only 3 days of exposure. After 6 days, the oxygen contamination is still the same, but after 20 days, there is still more oxygen present.

Figure 9 presents the S 2p core-level region measured for these films of **1**. Whereas the 3- and 6-day-old films show spectral features identical to the freshly prepared film (Figure 5), the 20-day-old film has at least one new spectral component

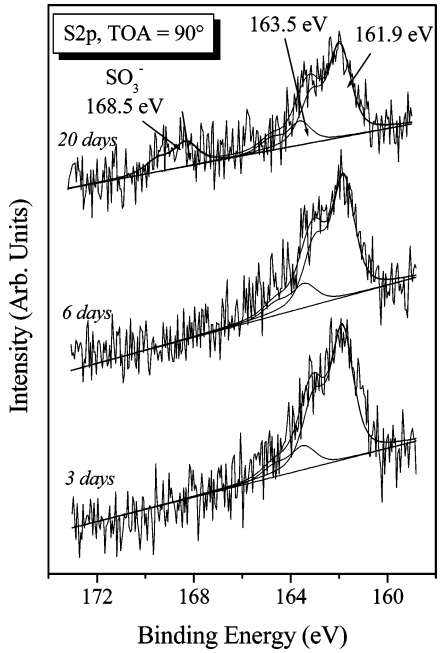

Figure 9. Photoemission spectra and fit of the S 2p core-level region for an 11-MUA film functionalized with macrocycle **1** recorded for different aging times in air.

at 168.5 eV binding energy that can be attributed to a sulfonite species (SO_3^-).[41] We can therefore conclude that the additional oxygen in the films exposed for 3 or 6 days is due to atmospheric contamination physisorbed onto the films and that after 20 days of aging the amount of oxygen still increases because of the oxidation of sulfur atoms. Nevertheless, the consistency in the N1s to S 2p, N1s to Au 4f, and S 2p to Au 4f ratios with time (Figure 8b) confirms that the macrocycle molecules are still intact on the SAM surface. Films of macrocycle **2** that were subjected to the same aging treatment showed a more rapid oxidation of sulfur than films of macrocycle **1**: in Figure 10, we show the S 2p core-level spectra recorded for the same film at different aging times. We can observe a weak peak at 168.5 eV indicating sulfur oxidation after 6 days of exposure to air. After 20 days of aging, the same peak represents a significant proportion of the total sulfur content of the film. The difference in the oxidation rate of the two types of macrocycle films can be explained on the basis of the difference in interaction with the SAM for chemically bonded **1** and physically adsorbed **2**: a different orientation of the macrocycles in the two cases or different homogeneities of these surfaces could allow for different channels for the oxygen penetration into the monolayer chains to reach the sulfur atoms. It is important to note that the stability of our functionalized surfaces against oxidation is in line with what is reported in the literature for CH_3-terminated SAMs with the same chain length as that of the alkanethiols used here.[41] Moreover, we observe that it is the component corresponding to the sulfur bonded to gold that decreases as the sulfonite species increases. The component with the S $2p_{3/2}$ peak at 163.5 eV remains unchanged, and this supports the attribution of the latter to disulfides. In fact, if noncovalently bound alkanethiols were present on the surface, then one would expect them to oxidize easier than the sulfur bonded to gold.[42]

The macrocycle **2** films were subjected to other types of stability tests to examine whether it was possible to substitute the macrocycle at the interaction site with the SAM with molecules containing functionality that can also interact with the SAM surface. Ammonium chloride ($NH_4^+Cl^-$) and aniline

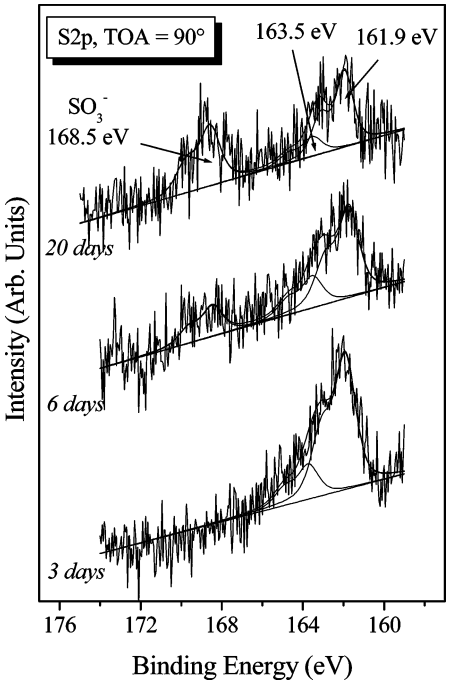

Figure 10. Photoemission spectra and fit of the S 2p core-level region for an 11-MUA film functionalized with macrocycle **2** recorded for different aging times in air.

TABLE 4: Comparison between Experimental Atomic Percentages Derived from the Photoemission Peak Areas of an 11-MUA Film Functionalized with Macrocycle 2 Freshly Prepared and after Immersion for Different Times in a 1 mM Methanol Solution of Aniline[a]

	freshly prepared	30 min aniline	3 h aniline	6 h aniline
%C	77.4 ± 1.5	78.1 ± 1.6	78.0 ± 1.6	78.4 ± 1.6
%O	15.9 ± 0.8	15.3 ± 0.8	15.4 ± 0.8	15.0 ± 0.8
%S	3.6 ± 0.4	3.1 ± 0.3	3.5 ± 0.4	3.6 ± 0.4
%N	3.2 ± 0.5	3.5 ± 0.5	3.1 ± 0.5	3.0 ± 0.5
N/S	0.9 ± 0.2	1.0 ± 0.2	0.9 ± 0.2	0.8 ± 0.1

[a] The error in the experimental atomic percentages was estimated to be 2% for C, 5% for O, 10% for S, and 15% for N.

(benzene-NH_2) were chosen because of their size and affinity for the acid-terminated SAM as appropriate candidates for substitution.

Macrocycle **2** films, prepared by 24 h of reaction with the SAM, were immersed in a 1 mM methanol solution of aniline for 30 min, 3 h, and 6 h. Table 4 presents the atomic percentages calculated from the XPS spectra recorded before and after this treatment. For all three reaction times, no changes in the nature of the functionalized surface can be seen. Moreover, the absolute values of the XPS peak areas indicate that no macrocycle **2** groups are lost from the surface. Analogous results were found when macrocycle **2** films prepared by 24 h of reaction with the SAM were immersed in a 15 mM aqueous solution of ammonium chloride for 1, 4, and 8 h. Moreover, for both series of treatments, we detect no changes in the N 1s core-level region; in the case of a displacement reaction taking place, we should observe new components at around 399 eV for hydrogen-bound amine groups or a new component at higher binding energy for a protonated ammonium nitrogen.[36]

These substitution tests indicate that the bond of macrocycle **2** with the SAM is stable and indirectly confirm our result for the functionalization yield in that it is only when the SAM surface is completely covered by **2** that the access of aniline or ammonium chloride molecules to the remaining free-acid terminal groups is sterically hindered.

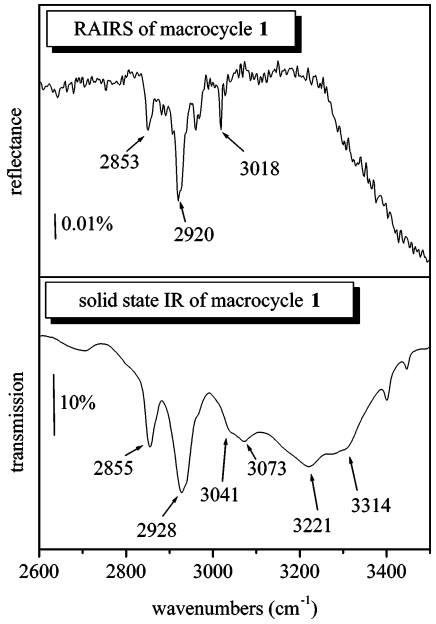

Figure 11. High-frequency RAIRS spectrum recorded at 2-cm^{-1} resolution of an 11-MUA film functionalized with macrocycle **1** (top panel) and transmission infrared spectrum recorded at 4-cm^{-1} resolution of 1 wt % macrocycle **1** in KBr (bottom panel).

TABLE 5: Assignments of Vibrational Modes for an 11-MUA Film Functionalized with Macrocycle 1 and the Solid-State Spectrum of 1 wt % Macrocycle 1 in KBr

	solid state (cm^{-1})	RAIRS (cm^{-1})
ν(NH)	3314	
ν(OH)	3221	
ν(CH)	3073	
ν(CH)	3041	3018
$\nu_{as}(CH_2)$	2928	2920
$\nu_{sym}(CH_2)$	2855	2853
ν(CO)	1756	1762
amide I	1641	1662
ν(CC)	1607	1611
amide II	1544	1533
ν(CC)	1509	1511
ν(CC)	1463	1452

d. RAIRS Measurements on Macrocycle 1. Because the grafting of macrocycle **1** seems to yield the most stable films with respect to aging in air, we decided to extend the analysis of this system using RAIRS to derive information on the orientation of the macrocycles with respect to the SAM surface plane.

The RAIRS spectrum obtained for the adsorbed macrocycle in the C−H stretching group frequency region is shown in Figure 11 (top panel). Although the absorption bands are inherently weak, it is possible to discern four features in the spectrum. The assignment of these bands is aided by comparison with the solid-state infrared transmission spectrum of **1** (Figure 11, bottom panel). The most important infrared absorption bands have been assigned[43] as detailed in Table 5. The most striking feature in the RAIRS spectrum is the appearance of a relatively intense band at 2920 cm^{-1}. This band can be unambiguously assigned to the CH_2 asymmetric stretching mode of the methylene groups in the octyl chain of the macrocycle and may also contain a contribution from the methylene units adjacent to the amide groups. The $\nu_{as}(CH_2)$ vibrational mode is generally

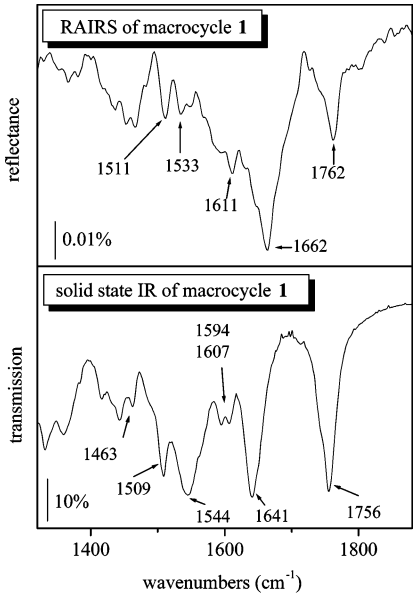

Figure 12. Low-frequency RAIRS spectrum recorded at 2-cm^{-1} resolution of an 11-MUA film functionalized with macrocycle **1** (top panel) and transmission infrared spectrum recorded at 4-cm^{-1} resolution of 1 wt % macrocycle **1** in KBr (bottom panel).

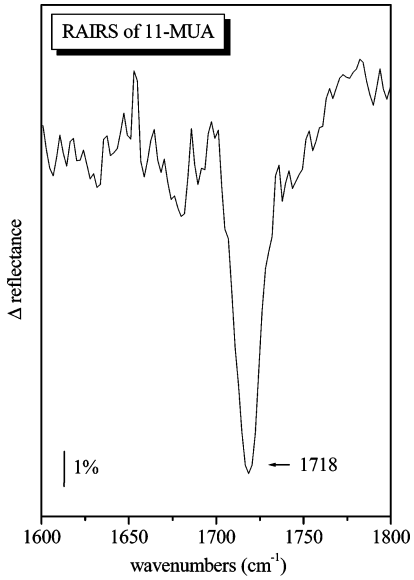

Figure 13. Carbonyl stretching region of the RAIRS spectrum recorded on an 11-MUA film on Au.

accompanied by a weaker CH_2 symmetric stretch at lower frequency,[43] and this band is observed in the spectrum at 2853 cm^{-1}.

The highest-frequency band in the C−H stretching region of the infrared spectrum occurs at 3018 cm^{-1}. The position of this band agrees with that expected for the C−H in-plane stretching mode of a phenyl ring,[44] and because macrocycle **1** contains phenyl groups, this is consistent with the presence of the macrocycle on the surface. The vibrational frequency for this mode is shifted down from the solid-phase frequency of 3041 cm^{-1} possibly because of the phenyl rings experiencing an interaction with the surface resulting in weakening of the carbon−hydrogen bonds in the phenyl rings. The final band in the spectrum observed at approximately 2960 cm^{-1} is an instrumental artifact due to instrumental instability and is not related to the macrocycle **1**/11-MUA system. Unfortunately, it was not possible to determine if the amide nitrogen−hydrogen stretch (expected between 3270 and 3330 cm^{-1} for the trans species[45]) is present in the RAIRS spectra because a broad absorption band due to ice condensing on the detector window obscures the region above 3100 cm^{-1}.

Further evidence for the presence of the macrocycle on the surface is provided by the RAIRS spectrum in the lower-frequency region as shown in Figure 12 (top panel), which we again compare to the solid-state infrared transmission spectrum of macrocycle **1** (Figure 12, bottom panel). The spectrum is rather complicated and contains a considerable number of absorption bands, but the most intense bands can be discerned. In the carbonyl stretching region, two infrared absorption bands are observed that provide strong evidence for the presence of amide functional groups on the surface: the most dominant peak at 1662 cm^{-1} corresponds to the amide I band (i.e., primarily a carbonyl stretch but also an in-phase bending of N−H and stretching of C−N of the amide functional group[46]). This band is accompanied by the amide II band (a C−N stretch combined with an N−H bend), which is observed as a weak feature at 1533 cm^{-1}. The carbonyl band at 1762 cm^{-1} is assigned to the carbonyl stretch of the ester functional group contained within the macrocycle.[47] Weak bands are observed at 1611 and 1511 cm^{-1}, and a very weak, broad feature is centered around 1452 cm^{-1}. The carbon−carbon stretching frequencies for 1,4-substituted phenyl rings normally occur in the regions of 1620−1585, 1590−1565 (weak), 1525−1480, and 1400−1420 cm^{-1} [43] and close to 1612 and 1460 cm^{-1} for 1,3,5-substituted phenyls.[47] Therefore, we deduce that the bands observed in the spectrum are due to both 1,4- and 1,3,5-substituted phenyl groups at the surface, as expected for the macrocycle grafted on the surface.

If the RAIRS spectra agree with the XPS data concerning the presence of **1** on the surface, the question still remains as to the nature of the interaction of the macrocycle with the self-assembled monolayer of 11-MUA. Because macrocycle **1** is expected to react with 11-MUA upon activation with EDCI to form a chemical attachment via an ester function, it should be possible to observe the ester in the RAIRS spectra. Clearly, we do observe an absorption band indicative of an ester group at 1762 cm^{-1} in the RAIRS spectrum, but this is due not only to a possible ester group between the macrocycle and 11-MUA but also to the ester functions within the macrocycle itself because both ester functions are in an identical chemical environment. Consequently, it is impossible to differentiate them using vibrational spectroscopy. An alternate approach to determine whether covalent attachment occurs between the macrocycle and 11-MUA is via monitoring the intensity of the carbonyl stretch of the carboxylic acid. Reaction between the macrocycle hydroxyl group and the acid group of 11-MUA effectively reduces the number of free acid groups at the surface. Because the RAIRS spectra are the ratio of the single-beam spectrum of the adsorbed macrocycle to that of 11-MUA on gold, we would therefore expect to see an anti-absorption band at the vibrational excitational frequency of the acid group. The most intense absorption band of the acid function is the carbonyl stretching mode of 11-MUA, which occurs at 1718 cm^{-1} for 11-MUA adsorbed on polycrystalline gold as shown in Figure 13, in agreement with ref 48. An examination of the spectrum reveals no evidence of an anti-absorption band in this region. However, this may be obscured by the absorption band due to the ester functional group occurring at 1762 cm^{-1}.

Additional interesting information concerning the adsorption geometry of the macrocycle can be obtained from vibrational spectroscopy. A comparison of the RAIRS spectra to the solid-state spectrum reveals that there is a marked difference in the relative intensity of the absorption bands. For a given poly-

crystalline solid sample, intensities of absorption bands depend only on the change in dipole moment associated with the vibrational mode. RAIRS absorption band intensity for adsorbates on a metal surface, however, is strongly influenced by the orientation and magnitude of the change in dipole moment of the vibration by consideration of the metal surface selection rule.[49] Vibrational modes that undergo a change in dipole moment with a large component parallel to the underlying metal will have weaker absorption bands than those with a large component perpendicular to the metal. Whereas the intensities of the amide I band (1662 cm^{-1}) and the carbonyl stretch of the ester (1762 cm^{-1}) are similar in the solid-state spectrum (Figure 12, bottom panel), the intensity of the ester is considerably weaker than that of the amide absorption band in the RAIRS spectrum (Figure 12, top panel). Consequently, the carbonyl groups of the esters (those within the macrocycle and, if they exist, those formed between the macrocycle and the surface) must be orientated such that the change in dipole moment associated with the carbonyl stretch has a smaller component perpendicular to the plane of the underlying gold surface. Therefore, on average, the ester groups must be angularly aligned so that the carbonyl groups are closer to the plane of the gold than the amide carbonyl groups.

The intensity of the in-plane C−H stretching mode of the phenyl ring for the RAIRS spectrum in Figure 11 (top panel) was observed to diminish with respect to the CH_2 stretching modes when compared to the solid-state spectrum (Figure 11, bottom panel). RAIRS studies of low coverages of benzene adsorbed on Cu(110) and Pt(111)[50] demonstrate that benzene adsorbs with the plane of the ring parallel to the plane of the metal and that the C−H stretching mode is strongly infrared-inactive. An examination of Figure 11 reveals that for macrocycle **1** adsorbed on 11-MUA the in-plane stretch is not disallowed but is observed as an extremely weak band. Hence, we can conclude that all three phenyl rings of the macrocycle are not orientated parallel to the plane of the underlying gold surface but some or all must exhibit some amount of tilt with respect to the metal surface. The observation of the weak carbon−carbon stretching bands in Figure 12 supports this assertion. The ν(CC) modes in 1,4- and 1,3,5-substituted phenyl groups result in a change in dipole moment associated with the vibration that is in-plane. Therefore, there must be some tilt of the rings with respect to the surface for the vibrational modes to be infrared-active. We note that this geometry of **1** is different from what is found for a benzylic amide macrocycle directly adsorbed onto a Au surface.[30]

4. Conclusions

We have established that macrocycles, the basic units of more complex mechanically interlocked architectures such as catenanes and rotaxanes, can be grafted onto acid-terminated SAMs by either chemical modification or physical adsorption, with the possibility to control the portion of functionalized surface area in both cases by varying the immersion time for the functionalization step. The two methods allow one to functionalize up to 30 or 40% of the acid groups on the SAM surface. This coverage appears quite important if we compare the dimensions of the acid groups with those of the macrocycles. If one wants to avoid intermolecular hydrogen bonding interactions that could hamper intramolecular motion, a functionalization of 40% represents the upper limit (i.e., the whole 11-MUA monolayer surface covered by **2**) if one considers that the orientation of the macrocycles on the surface may well be random.

From the photoemission spectra, we obtained no clear evidence for the type of interaction between the macrocycles and the SAM because of the complexity of the spectral regions comprising details of carbon and oxygen atoms involved in the interaction. Therefore, we checked a posteriori the stability of the interaction of the prepared films under different chemical or physical conditions. The films of **1** prepared by chemical bonding were tested by ultrasound treatment and with respect to aging in air and were proven to be stable. The films of **2** prepared by physical adsorption were also subjected to ultrasound treatment and demonstrated high stability. They are, however, less resistant than **1** to aging in air because they show incipient sulfur oxidation after only 6 days. Physisorbed macrocycle **2** was also tested against chemical substitution and was found to be stable.

The RAIRS spectra also provided evidence for the grafting of macrocycle **1** intact onto the surface. Moreover, a consideration of the relative absorption band intensities revealed that the ester carbonyl groups are on average oriented closer to the surface plane than the amide carbonyl groups and that the phenyl rings must have some degree of tilt with respect to the surface.

The encouraging results obtained for these macrocycles provide the basis for the grafting of more complex catenanes and rotaxanes using a similar approach.

Acknowledgment. We thank Dr. C. M. Whelan for a critical reading of the manuscript. This work was performed within the EU-TMR networks ENBAC (contract no. ERBFMRX-CT96-0059) and DRUM (contract no. ERBFMRX-CT97-0097) and with additional funding from the EU contract MECHMOL no. IST-2001-35504 and from the Belgian Interuniversity Program on Reduced Dimensionality Systems (PAI/IUAP 4/10) initiated by the Belgian Office for Scientific, Cultural and Scientific Affairs (OSTC).

References and Notes

(1) *Molecular Catenanes, Rotaxanes and Knots*; Sauvage, J.-P., Dietrich-Buchecker, C., Eds. Wiley-VCH: Weinheim, Germany, 1999.
(2) Amabilino, D. B.; Stoddart, J. F. *Chem. Rev.* **1995**, *95*, 2725.
(3) Barbara, P. F. *Acc. Chem. Res.* **2001**, *34*, 409 (special issue on molecular machines).
(4) Leigh, D. A.; Murphy, A. *Chem. Ind.* **1999**, *5*, 178.
(5) Bissell, R. A.; Córdova, E.; Kaifer, A. E.; Stoddart, J. F. *Nature* **1994**, *369*, 133.
(6) Anelli, P. L.; Spencer, N.; Stoddart J. F. *J. Am. Chem. Soc.* **1991**, *113*, 5131.
(7) Lane, A. S.; Leigh, D. A.; Murphy, A. *J. Am. Chem. Soc.* **1997**, *119*, 11092.
(8) Johnston, A. G.; Leigh, D. A.; Pritchard, R. J.; Deegan, M. D. *Angew. Chem., Int. Ed. Engl.* **1995**, *34*, 1209.
(9) Johnston, A. G.; Leigh, D. A.; Nezhat, L.; Smart, J. P.; Deegan, M. D. *Angew. Chem., Int. Ed. Engl.* **1995**, *34*, 1212.
(10) Leigh, D. A.; Moody, K.; Smart, J. P.; Watson, K. J.; Slawin, A. M. Z. *Angew. Chem., Int. Ed. Engl.* **1996**, *35*, 306.
(11) Leigh, D. A.; Murphy, A.; Smart, J. P.; Slawin, A. M. Z. *Angew. Chem., Int. Ed. Engl.* **1997**, *36*, 728.
(12) Johnston, A. G.; Leigh, D. A.; Murphy, A.; Smart, J. P.; Deegan, M. D. *J. Am. Chem. Soc.* **1996**, *118*, 10662.
(13) Ferretti, S.; Paynter, S.; Russell, D. A.; Sapsford, K. E.; Richardson, D. J. *Trends Anal. Chem.* **2000**, *9*, 19.
(14) Allara, D. *Biosens. Bioelectron.* **1995**, *10*, 771.
(15) Higashi, N.; Takahashi, M.; Niwa, M. *Langmuir* **1999**, *15*, 111.
(16) Madoz, J.; Kuznztzov, B. A.; Medrano, F. J.; Garcia, J. L. ; Fernandez, V. M. *J. Am. Chem. Soc.* **1997**, *119*, 1043.
(17) Blonder, R.; Willner, I.; Buckmann, F. *J. Am. Chem. Soc.* **1998**, *120*, 9335.
(18) Jordan, C. E.; Frey, B. L.; Kornguth, S.; Corn, R. M. *Langmuir* **1994**, *10*, 3642.
(19) Ostuni, E.; Yan, L.; Whitesides, G. M. *Colloids Surf., B* **1999**, *15*, 3.
(20) Gooding, J. J.; Hibbert, D. B. *Trends Anal. Chem.* **1999**, *8*, 18.

(21) Patel, N.; Davies, M. C.; Hartshorne, M.; Heaton, R. J.; Roberts, C. J.; Tendler, S. J. B.; Williams, P. M. *Langmuir* **1997**, *13*, 6485.

(22) Jiang, L.; Glidle, A.; Griffith, A.; McNeil, C. J.; Cooper, J. M. *Bioelectrochem. Bioenerg.* **1997**, *42*, 15.

(23) Yang, H. C.; Dermody, D. L.; Xu, C.; Ricco, A. J.; Crooks, R. M. *Langmuir* **1996**, *12*, 726.

(24) Strither, T.; Cai, W.; Zhao, X.; Hamers, R. J.; Smith, L. M. *J. Am. Chem. Soc.* **2000**, *122*, 1205.

(25) The SAM activation by the EDCI was performed both in water and in dichloromethane; for the same reaction times, the functionalization yield was more important in a water solution producing a stronger photoemission signal. For this reason, we choose to show the spectra recorded for a film prepared in water instead of the ones recorded for the film prepared in dichloromethane. However, the spectral analysis of the experimental data allowed the identification of the same components in both cases. We also note that because of the deprotonation of EDCI no high binding-energy peak characteristic of a protonated amine is found in either N 1s spectrum.

(26) Moulder, J. F.; Stickle, W. F.; Sobol, P. E.; Bomben, K. D. *Handbook of Photoelectron Spectroscopy*; Perkin-Elmer Corporation, Physical Electronics Division: Eden Prairie, MN, 1992.

(27) Czandema, A. W.; King, D. E.; Spauling, D. *J. Vac. Sci. Technol., A* **1995**, *9-5*, 2607.

(28) Vogt, A. D.; Han, T.; Beebe , T. B., Jr. *Langmuir* **1997**, *13*, 3397.

(29) Fustin, C. A.; Gouttebaron, R.; De Nadaï, C.; Caudano, R.; Zerbetto, F.; Leigh, D. A.; Rudolf, P. *Surf. Sci.* **2001**, *474*, 37.

(30) Whelan, C. M.; Cecchet, F.; Clarkson, G. J.; Leigh, D. A.; Caudano, R.; Rudolf, P. *Surf. Sci.* **2001**, *474*, 71.

(31) Arnold, R.; Azzam, W.; Terfort, A.; Wöll, Ch. *Langmuir* **2002**, *18*, 3980.

(32) We calculated the atomic percentages for many different coverages of the macrocycle but report here only the results for the functionalization of 12, 30, and 50% of the surface because these values correspond best to the experimental values.

(33) Wirde, M.; Gelius, U.; Dunbar, T.; Allara, D. L. *Nucl. Instrum. Methods Phys. Res., Sect. B* **1997**, *131*, 245.

(34) Heister, K.; Zharnikov, M.; Grunze, M.; Johansson, L. S. O.; Ulman, A. *Langmuir* **2001**, *17*, 8.

(35) Zharnikov, M.; Frey, S.; Heister, K.; Grunze, M. *Langmuir* **2000**, *16*, 2697.

(36) Beamson, G.; Briggs, D. *High-Resolution XPS of Organic Polymers: The Scienta ESCA Database*; Wiley & Sons: Chichester, U.K., 1992.

(37) Bureau, Ch. Private communication.

(38) Whelan, C. M.; Smyth, M. R.; Barnes C. J.; Brown, N. M. D.; Anderson C. A. *Appl. Surf. Sci.* **1998**, *134*, 144.

(39) Cecchet, F.; Leigh, D. A.; Gatti, F.; Margotti, M.; Paolucci, F.; Rapino, S.; Rudolf, P.; Wong, J. K. Y. To be submitted for publication.

(40) See, for example, Yan, L.; Marzolin, Ch.; Terfort, A.; Whitesides, G. M.; *Langmuir* **1997**, *13*, 6704.

(41) Li, Y.; Huang, J.; McIver R. T., Jr.; Hemminger, J. C. *J. Am. Chem. Soc.* **1992**, *114*, 2428. However, Schoenfisch and Pemberton (Schoenfisch, M. H.; Pemberton, J. E. *J. Am. Chem. Soc.* **1998**, *120*, 4502) report the incipient oxidation of the sulfur atoms after 4 h of aging, and after 24 h, all sulfur atoms are oxidized.

(42) Rieley, H.; Kendall, G. K.; Zemicale, F. W.; Smith, T. L.; Yang, S. *Langmuir* **1998**, *14*, 5147.

(43) Colthup, D. A.; Daly, L. H.; Wiberley, S. E. *Introduction to Raman and Infrared Spectroscopy*, 3rd ed.; Academic Press: New York, 1975.

(44) Wiberley, S. E.; Bunce, S. C.; Bauer, W. H. *Anal. Chem.* **1960**, *32*, 217.

(45) Cross, A. D. *Introduction to Practical Infrared Spectroscopy*; Butterworth: London, 1964.

(46) Theopharides, T.; Angiboust, J. F.; Manfait, M. *Spectroscopic and Structural Studies of Biomaterials I: Proteins*; Twardowski, J., Ed.; Sigma Press: Wilmslow, U.K., 1988.

(47) *Aldrich Library of Infrared Spectra*; Pouchert, C. J., Ed.; Aldrich Chemical Co.: Milwaukee, WI, 1981, Part 1.

(48) Sun, L.; Crooks, R. M.; Ricco, A. J. *Langmuir* **1993**, *9*, 1775.

(49) Only vibrations with a component of the dipole moment change normal to the surface may be observed.

(50) Haq, S.; King, D. A. *J. Phys. Chem.* **1996**, *100*, 16957.